Proposed dielectric-based microstructure laser-driven undulator

T. Plettner and R. L. Byer
Stanford University, Stanford, California 94305, USA
(Received 18 April 2007; published 20 March 2008)

We describe a proposed all-dielectric laser-driven undulator for the generation of coherent short wavelengths and explore the required electron beam parameters for its operation. The key concept for this laser-driven undulator is its ability to provide phase synchronicity between the deflection force from the laser and the electron beam for a distance that is much greater than the laser wavelength. Because of the possibility of high-peak electric fields from ultrashort pulse lasers on dielectric materials, the proposed undulator is expected to produce phase-synchronous GV/m deflection fields on a relativistic electron bunch and therefore lead to a very compact free electron based radiation device.

DOI: 10.1103/PhysRevSTAB.11.030704 PACS numbers: 41.60.Cr, 41.75.Jv, 41.75.Ht, 42.25.Bs

I. INTRODUCTION

The proposed undulator device is motivated by the possibility of future dielectric-based laser-driven particle accelerators that are expected to produce GeV/m acceleration gradients accompanied by a low-emittance, low-energy spread, and high-repetition rate attosecond electron pulses [1–6]. Development efforts for ultralow emittance [7] and optically bunched electron sources [8,9] as well as for dielectric-structure laser-driven particle accelerators are underway [10–13], and although these technologies are presently not mature, the possibility of a compatible undulator device that takes advantage of the ultrashort electron pulse structure appears worthwhile to explore.

Besides the proposed dielectric accelerator-undulator scheme several different advanced free-electron radiation concepts for ultrashort coherent wavelength generation are being investigated. For example, active undulators formed by very intense free-space waves inside optical resonators [14] or delivered by multiterawatt to petawatt laser systems [15] have been proposed. Furthermore microwave-cavity based active undulators are also being investigated [16,17]. Finally plasma wakefield accelerators [18–20] and laser-driven optical bunchers [21–23] are being considered as high-peak current, ultrashort pulse electron sources that feed into permanent-magnet undulators. The distinguishing feature of the undulator proposed here is that this is an active all-dielectric microstructure with an undulator period independent and much longer relative to the driving laser wavelength, and whose design is focused for operation with moderate power, high-repetition rate compact lasers. The proposed dielectric-structure accelerator-undulator system is not targeted for large electron bunch charges and high-peak x-ray pulses, but instead attempts to exploit the advantage of small tabletop mode-locked lasers capable of MHz repetition rates to generate similar x-ray photon repetition rate from a meter-scale footprint device.

The electron source for the proposed undulator is ideally a dielectric-structure laser-driven particle accelerator. Such an accelerator is an optical microstructure device that includes an electron beam vacuum channel with a geometry designed to couple a laser beam into an accelerating force that remains overlapped with the relativistic electron bunch traveling inside the vacuum channel. The dielectric substrate of the structure allows for application of high-peak power near-infrared laser beams [24,25] and when operated with few-femtosecond pulses is expected to support multi-GV/m peak electric fields that result in few-GeV/m acceleration gradients. This opens the possibility for GeV-energy electron beams from a few-meter accelerator structure.

Similar to rf accelerators, the longitudinal electric field component from a confined electromagnetic wave provides the accelerating force, and the structure geometry is designed such that this force remains phase synchronous with the relativistic particle. Some rf accelerators are capable of producing electron beams with a fractional energy spread of $\Delta\gamma/\gamma < 10^{-4}$ and a bunch length $c\tau_b \sim 10^{-4}\ \lambda_{\mathrm{EM}}$, where λ_{EM} is the wavelength of the driving electromagnetic wave [26]. Structure-based laser-driven particle accelerators operate by the same acceleration principle and are therefore expected to accomplish comparable energy spread and fractional bunch duration values. However, since the wavelength from near-infrared 1 μm lasers is scaled down by 4 orders of magnitude electron bunches with durations in the few-attosecond range become a possibility. This represents a major motivation for exploring an undulator that could be placed downstream of such a future attosecond GeV electron source. Electron injectors that deliver such electron beams do not exist at the present time, but research on optically driven attosecond electron emitters [8,9] and on low-energy attosecond bunchers [27] is taking place.

The reduction of the spatial features of the accelerator structure to submicron dimensions scales down the possible transverse electron bunch dimensions to similar values. It has been estimated that transverse normalized emittance values on the order of 10^{-9} m rad will be re-

quired for efficient transport of such electron beams through these structures [4,28,29]. The miniaturization and the ultralow-emittance requirements come at the expense of the possible bunch charge that can be supported by these accelerators. The loss factors from these structures are estimated to lie in the 100 GeV/m/pC range and thus only allow for maximum bunch charges in the fC range [30].

Not surprisingly, the successful implementation of these accelerators lies in the future. However, if this technology is proven a meter-long dielectric-based laser particle accelerator could deliver an already optically bunched GeV energy electron beam with attosecond pulse structure into an undulator. If a tabletop system is sought a matching compact undulator will be highly desirable. To this end we propose a dielectric microelectromechanical systems (MEMS)-based undulator structure that consists of laser-driven deflection elements and has electron beam transport requirements that match those of structure-based laser-driven particle accelerators. The key property of the proposed dielectric undulator is that the deflection force delivered from the laser beam inside the structure is phase synchronous with the electron beam. This allows the undulator period to be independent and for our purpose much longer than the wavelength of the driving laser.

We first describe the basics of the principle of laser-driven particle deflection that forms the basic building block of the proposed undulator. This is followed by the description of a possible quartz-based undulator structure that can be manufactured with existing microfabrication technology. Next, the maximum deflection force that is possible for this dielectric undulator is calculated. Finally, the requirements for FEL operation from the proposed undulator are discussed with an assumed set of electron beam parameters from a laser-driven particle accelerator.

II. THE ARCHITECTURE OF PROPOSED UNDULATOR STRUCTURE

A planar undulator with a period λ_u that exerts a deflection force of amplitude $F_\perp$ that varies sinusoidally with path length on a relativistic electron has an undulator parameter K of the form

$$K = \frac{2\pi\lambda_u}{mc^2} F_\perp. \tag{1}$$

A free-space electromagnetic wave interacting linearly with a free relativistic particle produces an effective undulator period λ_u that is comparable to the wavelength λ of the electromagnetic wave, that is, $\lambda_u \sim \lambda$. In contrast, for the proposed undulator we seek a condition that allows the optical near-field to generate a deflection force with an effective undulator period that satisfies $\lambda_u \gg \lambda$ and thus brings about a corresponding enhancement of K. The operation principle of the proposed dielectric laser-driven undulator is similar in many respects to that of dielectric-structure laser-driven particle accelerators. However, in addition to providing an acceleration force the proposed undulator can also generate an additional phase-synchronous deflection force whose direction is deliberately reversed externally at regular intervals to form the undulator.

To attain extended phase synchronicity between the laser electromagnetic wave and the relativistic electron bunch, we explore the concept of introducing a periodic phase modulation equal to the wavelength of the electromagnetic field near the particle trajectory. Laser-driven particle accelerators that employ this principle have been proposed in the past [4,5]. The same concept is applied here to find the conditions that lead to phase-synchronous particle deflection. A perspective view of a section of the proposed deflection structure is illustrated in Fig. 1(a). The

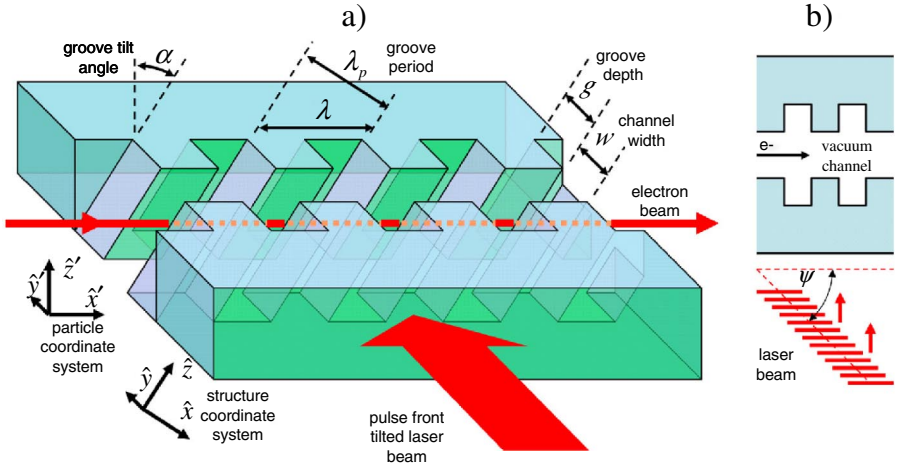

FIG. 1. (Color) (a) Perspective view of a section of the proposed deflection structure element. (b) Top view of a section of the structure. While the periodic grooves maintain phase synchronicity, the laser pulse-front tilt guarantees synchronicity of the laser pulse envelope with the relativistic electron bunch traveling in the vacuum channel.

grooves introduce a periodic phase modulation of the electromagnetic field in the vacuum channel that is responsible for the extended phase-synchronicity condition with the electron beam. The period of the vacuum channel grooves, denoted by λ_p in Fig. 1, is chosen such that its projection on the electron beam propagation axis equals the laser wavelength λ such that $\lambda_p = \lambda\cos\alpha$. The key element that enables this specific structure to provide a synchronous nonzero deflection force from the laser electromagnetic wave is the orientation of the periodic grooves of the vacuum channel. As shown in Fig. 1 these lie at an angle α with respect to the electron beam trajectory.

To analyze the laser-electron interaction in this structure, it is convenient to introduce two coordinate systems; one that is aligned to the structure grooves $(\hat{x}, \hat{y}, \hat{z})$, and another that is aligned to the electron beam trajectory $(\hat{x}', \hat{y}', \hat{z}')$. The laser beam is a plane wave with the phase front at normal incidence to the structure, traveling in the $\hat{x}$-direction. If the incoming laser beam is an ultrashort pulse its envelope has to be tilted to maintain overlap with the electron traveling inside the vacuum channel, as is shown in Fig. 1(b). The envelope tilt, known as pulse-front tilt, is a separate condition that is not to be mistaken for the orientation of the phase-front of the incoming wave. The particle is assumed to have a uniform, time-independent velocity $v \sim c$ and the structure is approximated by having infinite extent in the z-direction. In the coordinate system of the structure the particle's velocity is $\vec{v} = c(\cos\alpha\hat{y} + \sin\alpha\hat{z})$.

A configuration of this type, where the periodic groove direction is oriented at an angle to the electron beam, satisfies the phase-synchronicity condition for a nonzero deflection force acting on a speed-of-light particle [31]. This can be understood by first considering the special case, where the input laser field is monochromatic and has its magnetic field component aligned with the grooves in the $\hat{y}$-axis (a TM-polarized wave). For such a polarization, the nonzero field components inside the vacuum channel are E_x, E_y, and B_z. Because of the periodicity of the structure, the field components inside the vacuum channel are also periodic [32]. A TM plane wave at normal incidence on the structure generates field components along the electron beam trajectory inside the vacuum channel that have the form

$$\begin{aligned} E_x(x,0,z,t) &= \sum_{n=-\infty}^{+\infty} U_n e^{ink_p x} e^{ikct - i\phi} \\ E_y(x,0,z,t) &= \sum_{n=-\infty}^{+\infty} V_n e^{ink_p x} e^{ikct - i\phi} \\ B_z(x,0,z,t) &= \sum_{n=-\infty}^{+\infty} W_n e^{ink_p x} e^{ikct - i\phi}, \end{aligned} \tag{2}$$

where $k_p = 2\pi/\lambda_p$ and $k = 2\pi/\lambda$. The coefficients for which $n = 0$ represent the 0th transmission order through the structure which is a plane wave. The other orders create the field modulation that we are interested in. Inside the vacuum channel the time harmonic fields E_x, E_y, and B_z are related by Maxwell's equations in vacuum and the Fourier coefficients of E_y and B_z are found to be related by

$$V_n = -\frac{nk_p}{k/c} W_n. \tag{3}$$

The particle's trajectory is described by $\vec{r}(t) = (ct\cos\alpha, 0, ct\sin\alpha)$ and the particle's velocity vector is given by $\vec{v}(t) = c(\hat{x}\cos\alpha + \hat{z}\sin\alpha)$. Hence, the average force components can be described in terms of the Fourier coefficients

$$\begin{aligned} \langle F_x\rangle &= q\,\mathrm{Re}\left(\frac{1}{\lambda}\int_0^{\lambda}\sum_{n=-\infty}^{+\infty} U_n e^{is(k_p n\cos\alpha + k) - i\phi} ds\right) \\ \langle F_y\rangle &= q\,\mathrm{Re}\left(\frac{1}{\lambda}\int_0^{\lambda}\sum_{n=-\infty}^{+\infty} (V_n - c\cos\alpha W_n) e^{is(k_p n\cos\alpha + k) - i\phi} ds\right) \\ \langle F_z\rangle &= 0, \end{aligned} \tag{4}$$

where due to the oblique trajectory of the electron beam with respect to the grating its path length in one structure period λ_p equals the laser wavelength λ and is given by $\lambda = \lambda_p/\cos\alpha$ [see Fig. 1(a)]. The term $e^{-i\phi}$ is a constant that represents the optical phase of the particle with respect to the field and can be taken out of the path integral. For the possibility of $\langle F_x\rangle$ and $\langle F_y\rangle$ to be nonzero, there has to be one order n in the sum of Eq. (4) that possesses a non-oscillatory term, that is,

$$nk_p + k/\cos\alpha = 0. \tag{5}$$

When this condition is satisfied for the nth coefficient in Eq. (6), the average deflection gradient simplifies to

$$\langle F_y\rangle/q = \mathrm{Re}(e^{-i\phi} W_n)\sin^2\alpha. \tag{6}$$

Equation (6) establishes that a continuous, phase-synchronous deflection force can be produced by a monochromatic plane wave impinging on a periodic structure at normal incidence. Notice that when the tilt angle α between the particle trajectory and the structure is zero the phase-synchronous deflection force $\langle F_y\rangle$ vanishes. This establishes the necessity for a nonzero tilt angle for the specific deflection structure proposed here. A similar condition that requires $\alpha \neq 0$ for a nonzero phase-synchronous deflection force is also found to apply for the orthogonal polarization. The force components of Eq. (4) are specified in the (x, y, z) structure coordinates. However, we are interested in expressing these in the particle's coordinate system (x', y', z') by applying a rotation α about the y-axis:

$$\begin{aligned}\langle F_{x'}\rangle &= \langle F_x\rangle\cos\alpha + \langle F_z\rangle\sin\alpha \equiv \langle F_{\mathrm{acc}}\rangle \\ \langle F_{z'}\rangle &= -\langle F_x\rangle\sin\alpha + \langle F_z\rangle\cos\alpha \equiv \langle F_{\perp,z'}\rangle \\ \langle F_{y'}\rangle &= \langle F_y\rangle \equiv \langle F_{\perp,y'}\rangle,\end{aligned} \tag{7}$$

where $\langle F_{\mathrm{acc}}\rangle$ is the average acceleration force experienced by the particle and $\langle F_{\perp,y'}\rangle$ and $\langle F_{\perp,z'}\rangle$ are the average horizontal and vertical deflection forces, respectively. The total deflection force experienced by the particle is $\langle F_\perp\rangle = (\langle F_{\perp,y'}\rangle^2 + \langle F_{\perp,z'}\rangle^2)^{1/2}$.

The laser-driven deflection forces from periodic structures can also be generated with oblique incidence plane waves and pulse-front tilted laser beams, which are a linear superposition of monochromatic plane waves where the propagation direction of the particular plane wave is related to its wavelength [33]. For such laser beams it is found that, in addition to the phase-synchronicity condition for the center wavelength described by Eq. (5), a pulse-front tilt angle $\tan\psi = 1/\cos\alpha$ is required for maintaining overlap of the pulse envelope with the particle traveling inside the vacuum channel. A proof that includes these generalized aspects is presented elsewhere [31].

Cascaded sections of the proposed laser-deflection structure with M_u grating periods may form an undulator if the sign of the deflection force from the laser is alternated between the individual sections, resulting in an undulator period λ_u that corresponds to two such structure sections; $\lambda_u = 2M_u\lambda$. For a laser wavelength of $\lambda \sim 1$ μm and an undulator period $\lambda_u \sim 1$ mm, each section includes several hundred grating periods and is ideally powered by a separate laser beam whose optical phase and polarization are tuned to provide the desired sign of the force. For a dedicated deflection structure it is desirable to cancel the longitudinal force component, and linear superposition of separate input laser beams on the dielectric structure can provide such a condition [31]. However, due to the large loss factor in these narrow-aperture structures, an additional laser-driven acceleration force that accompanies the deflection force and counters the deceleration from longitudinal wakefields in the structure will be highly desirable.

III. A DIELECTRIC-BASED LASER-DRIVEN UNDULATOR STRUCTURE

A specific structure example that delivers a significant deflection gradient is discussed in this section. Crystalline dielectric materials that can be micromachined are ideal substrates for the proposed undulator. Besides the ability for microfabrication, the physical properties of the material in question determine its suitability. Key factors for a choice of a specific material include its chemical stability, melting point, thermal conductivity, and the index of refraction. For example, synthetic diamond possesses a very high thermal conductivity and high index of refraction but decomposes to graphite at relatively low temperatures and is difficult to manufacture. Sapphire or yttrium oxide also possess large indices of refraction and have high melting points but feature lower thermal conductivities. Certain oxides become chemically unstable in vacuum and chemically reduce in the presence of UV radiation. Fluorides such as MgF or CaF_2 possess the highest melting point and can withstand intense UV radiation in vacuum but have relatively low indices of refraction. In sum, the determination of the best-suited dielectric medium for an accelerator or undulator structure is a multifaceted problem in its own right and is a subject of separate study that lies beyond this concept proposal article. Although crystal quartz may not be the ultimate material of choice for this application, its nanofabrication technology is well developed and hence it is potentially an ideal substrate for future experiments aimed to test the conceptual ideas explored here. Quartz has an index of refraction of 1.58 at 800 nm, a band gap of 8.4 eV and as found with many other crystalline dielectric materials shows resistance to color center formation from high-energy photons and from neutrons [34]. Other high-band-gap materials like Y_2O_3, YAG, or SiC have higher indices of refraction but are more difficult to micromachine.

Consider a quartz-based undulator with a geometry as shown in Fig. 2(a), where the vacuum channel width w is chosen to be 0.4 λ and the other geometry parameters are optimized for a maximum deflection force. Numerical evaluation of the field components reveals that the maximum deflection is found to occur at a combination of groove depth $g = 0.85$ λ and a tilt angle $\alpha = 25°$. For these parameters, the deflection force is $\langle F_\perp/q\rangle \sim 0.15$ and the acceleration force is $\langle F_{\mathrm{acc}}/q\rangle \sim 0.3$, where the incoming wave is TM polarized and has a unit field amplitude $|E_{\mathrm{laser}}| = 1$. Comparable but slightly lower acceleration and deflection gradients are found for the opposite polarization.

The maximum gradient of the structure is set by the laser damage fluence of the material and local highest peak field intensity present anywhere in the structure. It is found that the maximum peak field amplitude occurs at the surface of

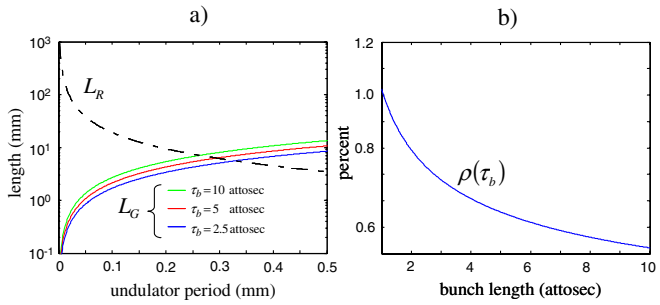

FIG. 2. (Color) (a) Rayleigh length L_R and one-dimensional FEL gain length L_{G0} versus undulator period for a 20 fC electron bunch λ_u. (b) FEL parameter ρ versus bunch duration τ_b for an undulator period of 0.3 mm and 20 fC bunch charge.

dielectric in the narrow region of the vacuum channel and is nearly 3 times the input laser amplitude; $|E_{\text{surface}}| \sim 3|E_{\text{laser}}|$. The maximum field is not to exceed the breakdown limit of the material, which depends on the laser wavelength and pulse format. The surface dielectric breakdown strength from ultrashort laser pulses with $\tau < 1$ psec has been observed to break the $\tau^{1/2}$ dependence seen with longer pulses and to remain near 1–2 J/cm^2 [24,25]. Assuming a damage fluence of 1 J/cm^2, the maximum applicable peak electric field from a 10 fsec laser pulse is approximately $|E_{\text{surface}}| \sim 27$ GV/m. Therefore the maximum input laser field amplitude is 3 times lower, and the corresponding acceleration and deflection force components take maximum values of $\langle F_{\text{acc}}/q\rangle \sim 2.7$ GV/m and $\langle F_{\perp}/q\rangle \sim 1.3$ GV/m. This laser-driven deflection effect corresponds to an equivalent magnetic deflection force of $\sim 4T$ on a relativistic charged particle.

IV. PARAMETERS PROPOSED FOR FEL OPERATION

The possibility of generation of FEL radiation from the proposed undulator is analyzed with a specific example of assumed electron beam parameters from a dielectric-structure laser-driven particle accelerator which are listed in Table I. As described in the Introduction, the electron beam from such accelerators is expected to show ultralow-emittance values and bunch durations in the attosecond regime. The bunch charge listed in Table I is derived with simple longitudinal beam loading considerations in the Appendix.

The acceptable length of the undulator and possible undulator period values are derived from electron beam, from photon beam transport considerations, and from the one-dimensional FEL conditions.

A. Beam transport through the dielectric undulator

The narrow aperture of the dielectric undulator determines the maximum possible electron spot size and bunch charge that can be transported through the structure. For simplicity a round beam is considered. As a beam transport criterion, the beam should be smaller than half the vacuum channel width shown in Fig. 2(a), which corresponds to a beam diameter of $D_0 \sim 200$ nm. Although periodic focusing for extended propagation of such beam diameters is possible, the present discussion will only consider simple beam drift inside a short undulator section whose practical length is limited by the electron and the photon beam expansion inside the undulator vacuum channel. Practical dimensions for a monolithic dielectric MEMS structure such as the proposed undulator are on the order of a few-cm in length. This sets a limit on the geometric emittance of the beam, whose focal depth β^* should be comparable to the length of the undulator if no periodic focusing is to be considered. Therefore β^* is to be longer than 1 cm and for the assumed electron beam diameter D_0 have a corresponding geometric emittance $\varepsilon_{\text{geom}} \sim D_0^2/4\beta^* \sim 10^{-12}$ m rad. Hence, for an electron beam with a normalized emittance of $\varepsilon_N \sim 10^{-9}$ m rad, a gamma factor of $\gamma > 10^3$ will be required for successful transport through the structure. In the remainder of this article, a specific electron beam energy of 2 GeV ($\gamma \sim 4 \times 10^3$) will be assumed. These beam parameters set β^* at ~ 4 cm. In addition to the electron beam transport, the propagation and spread of the photon beam has to be considered as well. As a coarse criterion, the Rayleigh range of the photon beam with a waist equal to the electron beam should be comparable to the β^* of the electron beam. The photon wavelength that satisfies a Rayleigh range $Z_R > 1$ cm and a beam waist of $\omega_0 \sim 10^{-7}$ m should be $\lambda_r < 2\pi\omega_0^2/Z_R \sim 10^{-10}$ m with a corresponding undulator period of $\lambda_u \sim 10^{-4}$ m. Finally, the maximum electron bunch charge is determined by the loss factor from the narrow-aperture structure. The Appendix presents an order-of-magnitude estimate for the loss factor of the configuration described here, which arrives at a value of ~ 100 GeV/pC-m and an allowable bunch charge of ~ 20 fC. As verified with general particle tracer (GPT) [35] an electron beam with parameters of Table I is emittance and not space charge dominated. GPT predicts that a tenfold increase in bunch charge is required to reduce β^* by a factor of 2 from space-charge effects.

TABLE I. Electron beam parameters expected for structure-based laser-driven particle accelerators.

Beam energy	2 GeV
Transverse emittance ϵ_N	10^{-9} m rad
Energy spread $\Delta\gamma/\gamma$	0.1%
Drive wavelength λ_{EM}	1 μm
Bunch duration τ_b	$\tau_b \sim 5$ attosec
Bunch charge	20 fC
Spot size	200 nm

B. Conditions from the one-dimensional FEL model

The emittance, gain length, and energy spread conditions for the one-dimensional FEL approximation can serve as a guide for determining the range of possible undulator period values compatible with FEL operation. First, the normalized emittance has to follow

$$\varepsilon < (\lambda_r/4\pi)\gamma. \tag{8}$$

For the target normalized emittance of $\varepsilon_N \sim 10^{-9}$ m rad, the radiation wavelength should satisfy $\lambda_r > 10^{-12}$ m. On the other hand, it was determined earlier that for a sufficiently long Rayleigh range $\lambda_r < 10^{-10}$ m. These two wavelength restrictions alone establish that $10^{-12} < \lambda_r < 10^{-10}$ m. This range is reduced further by the second one-dimensional FEL condition that requires the FEL gain length to be shorter than the Rayleigh range, namely,

$$L_G < L_R. \tag{9}$$

The gain length describes the inverse of the amplitude exponential growth rate and in the one-dimensional steady-state FEL model is given by

$$L_{G0} = \frac{\gamma}{\sqrt[3]{B^2 \lambda_u n_e}}. \tag{10}$$

Since the electron bunch charge and the electron spot size have been established to be ~20 fC and 200 nm, respectively, the bunch duration is the remaining free parameter to determine the particle density n_e in Eq. (10). As described earlier, structure loaded laser-driven particle accelerators can support electron bunch lengths of $\sim 1/10^3$ of the driving electromagnetic wave, and for 1 μm laser wavelengths this scales down to few-attosecond bunches. Figure 2(a) shows a plot of the FEL gain length $L_{G0}(\lambda_u)$ and the corresponding Rayleigh range $L_R(\lambda_u)$ plotted versus the undulator period at bunch durations of 2, 5, and 10 attosec. To satisfy the inequality of Eq. (9) undulator periods of $\lambda_u = 0.5$ mm or shorter are required. As a design example consider $\lambda_u = 0.3$ mm and $\tau_b = 5$ attosec, such that $L_R \sim 4L_{G0}$. Such a condition allows for some degradation of the effective gain length from field slippage and other factors.

Finally, the third one-dimensional FEL condition considered here requires that the fractional energy spread of the beam be smaller than the FEL parameter, that is, $\Delta\gamma/\gamma < \rho$. Figure 2(b) shows the corresponding FEL parameter ρ_{1D} expected from the one-dimensional FEL model as a function of the electron bunch duration for $\lambda_u = 0.3$ mm and the same electron beam parameters as in Fig. 2(a). It can be appreciated that to satisfy $\Delta\gamma/\gamma < \rho$ the required beam energy spread $\Delta\gamma/\gamma$ should be less than 0.5%. The target electron beam and undulator parameters for the proposed FEL operation are summarized in Table II and are employed to model the expected FEL growth.

TABLE II. Target electron beam, undulator, and photon parameters.

Electron beam parameters	
Beam energy	2 GeV
Transverse emittance	10^{-9} m rad
Energy spread	0.1%
Bunch duration	$\tau_b \sim 5$ attosec
Bunch charge	20 fC
Spot size	200 nm
Undulator parameters	
Undulator period	0.3 mm
Undulator strength K	0.14
Undulator length	12 cm (400 periods)
Photon parameters	
Wavelength	1.0×10^{-11} m
Photon energy	120 keV
Rayleigh range	25 mm

Slippage from the short electron bunch can be expected to significantly lengthen the effective gain length and to determine the FEL pulse shape emerging from the undulator. When the ratio of the bunch length σ_b to the cooperation length L_c is $\sigma_b/L_c < 2\pi$, the FEL process lies in the short pulse regime [36]. The cooperation length is given by $L_c = (\lambda_r/\lambda_u)L_{G0}$. A 5 attosec electron bunch traversing the proposed undulator has a length $\sigma_b \sim 136\ \lambda_r$, and with $L_{G0} \sim 7$ mm [see Fig. 2(a)] the cooperation length is $L_c \sim 21\ \lambda_r$. Hence, $\sigma_b/L_c \sim 6$ belongs to the short bunch regime that is dominated by slippage, where the FEL temporal structure is expected to feature a single smooth peak. Figure 3 illustrates the expected FEL pulse evolution from four different input electron bunches with the parameters of Table I at three different locations in the undulator. The FEL field evolution in Fig. 3 was modeled by numerical evaluation of the one-dimensional particle pendulum equations and the one-dimensional field envelope growth equation. The initial state of the electron bunch was specified by assigning initial energy and longitudinal phase offset coordinates for each particle in a Gaussian distribution.

As shown in Fig. 3(d) saturation is expected to be reached within ~550 undulator periods, which corresponds to ~25 gain lengths. At saturation 10^6 photons are expected, corresponding to an FEL pulse energy of ~20 nJ and an effective FEL parameter of $\rho_{\text{eff}} = U_{\text{FEL}}/U_{\text{beam}} \sim 5 \times 10^{-4}$. This saturation value is in agreement with the expected FEL parameter from the one-dimensional steady-state model shown in Fig. 2(b). However, the effective FEL growth rate in Fig. 3(d) is

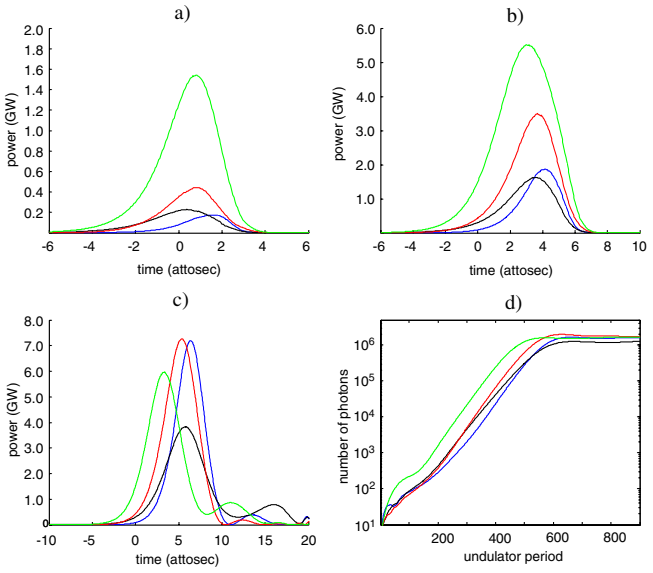

FIG. 3. (Color) Temporal FEL power profiles at (a) 400 undulator periods (12 cm), (b) 500 undulator periods (15 cm), and (c) 900 undulator periods (27 cm). (d) Integrated pulse energy expressed as total number of center-wavelength photons versus undulator period.

lower than that expected from the one-dimensional steady-state model and can be accounted for by the field slippage from the short electron bunch. Following semianalytical models that include longitudinal pulse structure, the effective gain length can be approximated by $L_G \sim L_{G0}(1 + N_s\lambda_r/3\sigma_b)$ [37], which results in $L_G \sim 2.1\ L_{G0}$ or 45 undulator periods with the assumed parameters. This is in agreement with slope of the FEL power growth curves shown in Fig. 3(d).

Finally, Figs. 3(a)–3(c) support the prediction from analytical models for the formation of a single FEL pulse with the parameters specified in Table I. Shorter undulators having 500 periods or less are expected to produce lower pulse energies with a wide shot-to-shot pulse energy jitter while undulators longer than the saturation length can be expected to produce a more uniform pulse intensity but with a larger timing jitter. In the absence of electron beam focusing, the undulator length will be limited to the transverse growth of the electron beam. With the vacuum channel width of twice the focused bunch diameter clipping of the electron beam from the undulator walls starts to occur with an undulator length of $L \sim 4\ \beta^*$, or 530 undulator periods. Therefore in the absence of focusing a maximum undulator length of ~400 periods or shorter is possible with the electron beam parameters of Table II.

Because of the fC-scale bunch charge, the photon flux from the proposed undulator is of $\sim 10^5$ photons per FEL pulse, 4 orders of magnitude below that of large-scale x-ray FEL facilities. However, the moderate-power solid-state lasers that are to power the proposed structure-based accelerator and undulator are compatible with MHz repetition rates and therefore allow for an integrated x-ray photon flux than can be comparable to that of large-scale facilities.

To summarize, the electron beam transport and FEL radiation conditions impose a narrow operating range both on the electron beam and on FEL radiation wavelengths possible with the proposed undulator. Beam transport considerations and the one-dimensional FEL conditions place an acceptable FEL radiation wavelength range of $10^{-12} < \lambda_r < 10^{-11}$ m and in the absence of beam focusing limit the acceptable undulator length to a few-cm. Except for the very short electron bunch duration, all other beam parameters in Table I were selected by employing the one-dimensional FEL model as a design guide, and the expected deviations from this model can be accounted for by the field slippage from the short electron bunch.

Finally, the expected high photon energy and low FEL parameter prompt the question of possible quantum effects on the SASE-FEL from the proposed system. However, despite the high photon energy the selected 2 GeV kinetic energy of the electrons is much higher and the fractional energy loss from recoil with the FEL photons becomes negligible. The quantum FEL parameter, defined by the ratio of the final momentum spread of the electron beam at saturation and the photon momentum recoil [38,39] serves as a guide for possible FEL operation in the quantum regime:

$$\bar{\rho} = \rho \frac{mc\gamma}{\hbar k_r}. \tag{11}$$

ρ is the classical FEL parameter that was estimated to be $\sim 5 \times 10^{-4}$, m is the electron mass, c is the speed of light, $\hbar$ is Planck's constant, and $k_r = 2\pi/\lambda_r$ the FEL photon wave number. The quantum FEL parameter resulting from the proposed photon and electron beam properties of Table II is $\bar{\rho} \sim 83$. Quantum effects become relevant when $\bar{\rho} \leq 1$, and in light of this the classical electrodynamics approach taken here seems an accurate description of the expected FEL process.

V. SUMMARY

This article described a possible tabletop FEL system that is entirely based on microstructure optical components. The main aspects that separate this concept from other existing or proposed FEL systems are the envisioned implementation of high-repetition rate moderate-power lasers and the use of dielectric microstructures that shape the electromagnetic fields for the manipulation of the free electrons, both for particle acceleration and for deflection in an all-dielectric undulator.

The large deflection gradients from the proposed laser-driven undulator and the possibility of attosecond-duration electron bunches caused by the driving wavelength could lead to a few-cm long undulator and for the possibility of generation of x rays with corresponding temporal pulse structure and photon energies in the hundred keV range from a meter-scale device. Although of lower pulse energy than large-scale FEL facilities, the MHz repetition rate will allow for a continuous pulse-train operation and circumvent the need for macropulse operation and low-repetition rate power cycling. Therefore noise sources from acoustic and heat transients introduced by power cycling could be entirely suppressed with the proposed system and, as is possible with solid-state lasers, further stabilization from active feedback systems with multi-kHz bandwidth becomes a natural possibility. In sum, the proposed FEL system is expected to possess an inherently better stability due to the possibility of quasi-cw operation.

VI. OUTLOOK

The proposed undulator was described for operation with electron beam parameters expected from future structure-based laser-driven particle accelerators. Since their development is in its infancy, their application dielectric-microstructure laser-driven particle accelerators with the proposed undulator is unlikely to become a reality in the near future. On the other hand, other more mature high-gradient accelerator technologies may function as

near-term electron test sources for the proposed undulator. One such technology is laser-driven plasma wakefield acceleration, which has accomplished dramatic improvements in its beam energy spread and emittance parameters to levels that now rival conventional rf accelerators [40]. Not surprisingly, there are experimental efforts to apply this particle accelerator technology as an electron source for permanent-magnet undulators [18–20]. These accelerators have been shown to produce bunches of >100 pC charge at 1 GeV energy having a femtosecond time structure within a centimeter distance [41]. These bunch charges are large enough to consider emittance and energy filtering to produce GeV electron bunches of few fC with parameters comparable to those of Table II that could be injected into a dielectric centimeter-long undulator to produce femtosecond x rays. Such a plasma-dielectric-structure hybrid that could be worthwhile in itself to explore further.

Although one particular scenario that is of interest to the authors was described in some depth, the ultimate design parameters for the proposed undulator will depend on their degree of success and on their limitations that are yet to be fully established. Nonetheless the prospect of generating coherent x-ray pulses from a microstructure based device powered by a high-repetition rate mode-locked laser system presents the possibility of an ultracompact free-electron based radiation device. Possible improvements to the presented system include concepts that are already under consideration for other FEL systems, such as recycling of the laser beam that powers the accelerator structure [42], resonating of the x-ray photons [43], or recycling of the electron beam such as proposed for future x-ray FELs driven by superconducting accelerators [44].

ACKNOWLEDGMENTS

The authors would like to thank R. Rice and H. Injeyan for their advice on possible future improvements to the proposed system and potential applications of an integrated laser-driven FEL device. We also appreciate valuable advice from P. Hommelhoff on the capabilities and limitations from laser-driven field emission sources and their possible application to particle accelerators. We also thank R. Ischebeck and Z. Huang for valuable advice on SASE FELs. This work is supported by Northrop Grumman Space Technology.

APPENDIX: ESTIMATE OF THE LOSS FACTOR

The deflection elements of the dielectric undulator are periodic structures and therefore the dominant radiation mechanism can be expected to be Smith-Purcell (SP) radiation, which can radiate into the vacuum channel or into the dielectric medium. The forward SP radiation, labeled as SP_1 in Fig. 4(a), has been analyzed by [45]. For this radiation mechanism to be effective the ratio between the height of the electron beam above the grating x_0 and the grating period λ_p have to follow

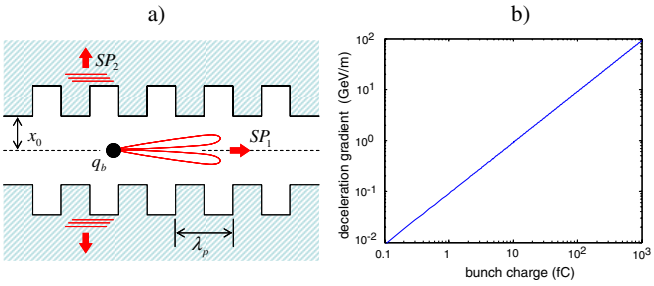

FIG. 4. (Color) (a) Schematic of the main possible radiation mechanisms for a periodic structure. (b) Approximate decelerating gradient versus bunch charge.

$$4\pi x_0/\lambda_p \sim 1/\gamma. \tag{A1}$$

The distance of the electron beam from the grating surface is $x_0 \sim 0.2\ \lambda_p$ and $\gamma \sim 4 \times 10^3$. Therefore the forward SP radiation mechanism is suppressed since $4\pi x_0/\lambda_p \gg 1/\gamma$. On the other hand, the SP radiation into the dielectric medium, labeled as SP_2 in Fig. 4(a), can be expected to dominate since the structure is designed to efficiently couple a laser beam from the dielectric medium to the electron beam in the vacuum channel. The SP_2 radiation is the inverse mechanism of the laser-electron interaction that was evaluated in Sec. II. For an order-of-magnitude estimate of the strength of SP_2, assume that the electron bream is a sheet beam of infinite extent having the electron density that corresponds to the assumed electron bunch charge in a beam diameter D. This two-dimensional model yields an overestimate of the coupling of the electron wakefields with the structure but allows for a simple analytical analysis based on energy balance considerations similar in spirit to those carried out for evaluation of longitudinal wakefields in resonant cavity structures [46,47]. Here the energy balance is applied to a section of the structure that covers a length L and a height D. For the simple two-dimensional geometry, the energy change on the electron beam over that drift distance L is equal to the net electromagnetic energy that flows into that volume of the structure:

$$qV = \frac{DL}{2Z_0}[E_L^2 - (E_L + E_W)^2]\tau_L, \tag{A2}$$

where E_L is the laser field amplitude, E_W the overlapping beam wakefield amplitude, and $\tau_L = L/c\beta$ is the drift time of the charge bunch for the length L. For a single electron, the wakefield is very small compared to the laser field; $E_W = -\xi E_L$, where $|\xi| \ll 1$. Therefore the term that scales as ${E_W}^2$ in Eq. (A2) can be neglected. In this limit the work is related to the unloaded laser-acceleration gradient G_1, which is proportional to the input laser field amplitude; $G_1 = T_{||}E_L$. Therefore the work from the laser

on a single electron is $W_1 = eV_1 = eG_1L$, and employing Eq. (A2) it can be rewritten as

$$W_1 = eV_1 = eG_1L = eT_{||}E_LL \sim \frac{\xi DL^2E_L^2}{c\beta Z_0}. \quad \text{(A3)}$$

Therefore the constant ξ can be expressed as

$$\xi = \frac{e\beta cT_{||}Z_0}{LDE_L}. \quad \text{(A4)}$$

For a bunch charge $q_b = Ne$ with N electrons, the total work on the bunch does include the beam loading term that scales as ${E_W}^2$ neglected in the derivation of Eq. (A3). For a bunch with N particles, the total wakefield is $E_W = -\xi NE_L$, and therefore the total work becomes

$$W_N = eNV_N = eNG_NL = \frac{DL}{2Z_0}(2N\xi E_L^2 - N\xi^2E_L^2)\tau_L. \quad \text{(A5)}$$

Hence, the effective loaded gradient G_N is

$$G_N = G_1 - \frac{T_{||}^2Z_0\beta c}{2DL}q_b \equiv G_1 - K_Lq_b, \quad \text{(A6)}$$

where K_L is the loss factor. For the proposed undulator structure, it was found in Sec. II that the acceleration gradient is $\sim$0.3 times the input laser field E_L, and hence $T_{||} = 0.3$. With the assumed electron beam diameter $D \sim 2 \times 10^{-7}$ m, the loss factor from radiating into one dielectric side at the TM polarization is $K_L \sim 25$ GeV/m-pC. However, since the electrons can radiate into the two dielectric sides and can also radiate with about the same coupling strength into the other polarization, the total loss factor is 4 times as large, namely $K_L \sim 100$ GeV/m-pC. Other dielectric accelerator structures that also transport submicron diameter electron bunches have been estimated to have similar loss factor values [30]. Figure 4(b) shows a plot of the decelerating gradient versus bunch charge. Requiring a beam loading condition where $K_Lq_b = G_1$ establishes a maximum bunch charge at which the deceleration of the bunch is canceled by the laser accelerating force. In Sec. II it was stated that the expected maximum unloaded acceleration gradient for the structure is $\sim$4 GeV/m and hence the maximum allowable bunch charge for which the net loaded gradient is zero is $q_b \sim$ 40 fC. Optimum beam loading occurs at half this charge. Therefore to study the conditions for FEL radiation from the dielectric undulator a bunch charge of $q_b \sim 20$ fC is assumed.

[1] Y. C. Huang, D. Zheng, W. M. Tulloch, and R. L. Byer, Appl. Phys. Lett. **68**, 753 (1996).
[2] X. Eddie Lin, Phys. Rev. ST Accel. Beams **4**, 051301 (2001).
[3] B. Cowan, Phys. Rev. ST Accel. Beams **6**, 101301 (2003).
[4] J. Rosenzweig, A. Murokh, and C. Pellegrini, Phys. Rev. Lett. **74**, 2467 (1995).
[5] T. Plettner, P. P. Lu, and R. L. Byer, Phys. Rev. ST Accel. Beams **9**, 111301 (2006).
[6] Z. Zhang, S. G. Tantawi, and R. D. Ruth, Phys. Rev. ST Accel. Beams **8**, 071302 (2005).
[7] J. W. Lewellen and J. Noonan, Phys. Rev. ST Accel. Beams **8**, 033502 (2005).
[8] P. Hommelhoff, Y. Sortais, A. Aghajani-Talesh, and M. A. Kasevich, Phys. Rev. Lett. **96**, 077401 (2006).
[9] P. Hommelhoff, C. Kealhofer, and M. A. Kasevich, Phys. Rev. Lett. **97**, 247402 (2006).
[10] T. Plettner, R. L. Byer, E. Colby, B. Cowan, C. M. S. Sears, J. E. Spencer, and R. H. Siemann, Phys. Rev. Lett. **95**, 134801 (2005).
[11] T. Plettner *et al.*, AIP Conf. Proc. **877**, 103 (2006).
[12] M. Lincoln *et al.*, AIP Conf. Proc. **877**, 859 (2006).
[13] E. Colby and P. Musumeci, AIP Conf. Proc. **877**, 183 (2006).
[14] Z. Huang and R. Ruth, Phys. Rev. Lett. **80**, 976 (1998).
[15] D. F. Gordon, P. Sprangle, B. Hafizi, and C. W. Roberson, Nucl. Instrum. Methods Phys. Res., Sect. A **475**, 190 (2001).
[16] S. Tantawi, V. Dolgashev, C. Nantista, C. Pellegrini, J. Rosenzweig, and G. Travish, *Proceedings of the 27th International Free Electron Laser Conference, Stanford, CA*, econf C0508213 (2005), pp. 438–441.
[17] K. Batchelor, *Proceedings of the 1986 Linear Accelerator Conference* (1986), pp. 272–275, http://adsabs.harvard.edu/abs/1986STIN...8631773B.
[18] C. B. Schroeder, W. M. Fawley, E. Esarey, and W. P. Leemans, *Proceedings of the 28th International Free Electron Laser Conference, Berlin, Germany* (2006), pp. 455–458, http://www.bessy.de/fel2006/proceedings/.
[19] D. A. Jaroszynski, R. Bingham, E. Brunetti, B. Ersfeld, J. Gallacher, B. van der Geer, R. Issac, S. P. Jamison, D. Jones, M. de Loos, A. Lyachev, V. Pavlov, A. Reitma, Y. Saveliev, G. Vieux, and S. M. Wiggins, Phil. Trans. R. Soc. A **364**, 689 (2006).
[20] F. Grüner *et al.*, Appl. Phys. B **86**, 431 (2007).
[21] Y. C. Huang and R. L. Byer, in *Proceedings of the 18th International Free Electron Laser Conference, Rome, Italy* (North-Holland, Amsterdam, 1997), Part II, pp. 37–38.
[22] A. A. Zholents and W. M. Fawley, Phys. Rev. Lett. **92**, 224801 (2004).
[23] A. A. Zholents and G. Penn, Phys. Rev. ST Accel. Beams **8**, 050704 (2005).
[24] M. Lenzner *et al.*, Phys. Rev. Lett. **80**, 4076 (1998).
[25] B. C. Stuart *et al.*, Phys. Rev. Lett. **74**, 2248 (1995).
[26] TESLA technical design report, part V, The X-Ray Free-Electron Laser (2001)
[27] E. Fill *et al.*, New J. Phys. **8**, 272 (2006).
[28] B. Cowan, SLAC-PUB-12090, 2006.
[29] B. Cowan, Phys. Rev. ST Accel. Beams **6**, 101301 (2003).
[30] R. H. Siemann, Phys. Rev. ST Accel. Beams **7**, 061303 (2004).
[31] T. Plettner, Report No. SLAC-PUB-12458, 2007.
[32] M. Nevière and E. Popov, *Light Propagation in Periodic Media* (Marcel Decker, Inc., New York, 2003), pp. 21–22.
[33] J. Hebling, Opt. Quantum Electron. **28**, 1759 (1996).

[34] E. Colby, G. Lum, T. Plettner, and J. Spencer, IEEE Trans. Nucl. Sci. **49**, 2857 (2002).
[35] General Particle Tracer (GPT), Pulsar Physics, http://www.pulsar.nl/.
[36] R. Bonifacio, L. De Salvo, P. Pierini, N. Piovella, and C. Pellegrini, Phys. Rev. Lett. **73**, 70 (1994).
[37] G. Dattoli, L. Giannessi, P. L. Ottaviani, and C. Ronsivalle, J. Appl. Phys. **95**, 3206 (2004).
[38] R. Bonifacio, G. R. Robb, N. Piovella, A. Schiavi, and L. Serafini, *Proceedings of the 27th International Free Electron laser Conference, Stanford, CA* (2005), pp. 71–74.
[39] R. Bonifacio, N. Piovella, G. R. Robb, and A. Schiavi, Phys. Rev. ST Accel. Beams **9**, 090701 (2006).
[40] C. G. R. Geddes, Cs. Toth, J. van Tilborg, E. Esarey, C. B. Schroeder, D. Bruhwiler, C. Nieter, J. Cary, and W. P. Leemans, Nature (London) **431**, 538 (2004).
[41] W. P. Leemans, B. Nagler, A. J. Gonsalves, Cs. Tóth, K. Nakamura, C. G. R. Geddes, E. Esarey, C. B. Schroeder, and S. M. Hooker, Nature Phys. **2**, 696 (2006).
[42] N. Na, R. H. Siemann, and R. L. Byer, Phys. Rev. ST Accel. Beams **8**, 031301 (2005).
[43] Z. Huang and R. Ruth, Phys. Rev. Lett. **96**, 144801 (2006).
[44] J. Sekutowicz *et al.*, Phys. Rev. ST Accel. Beams **8**, 010701 (2005).
[45] K. J. Woods, J. E. Walsh, R. E. Stoner, H. G. Kirk, and R. C. Fernow, Phys. Rev. Lett. **74**, 3808 (1995).
[46] P. B. Wilson, Report No. SLAC-PUB 4547, 1989.
[47] K. L. F. Bane and G. Stupakov, Phys. Rev. ST Accel. Beams **6**, 024401 (2003).